Publisher's version: Irvine DJ, Kurylyk BL, Briggs MA. 2020. Quantitative guidance for efficient vertical flow measurements at the sediment-water interface using temperature-depth profiles. Hydrological Processes, 34(3): 649-661. DOI: 10.1002/hyp.13614.

Note: This is the accepted version of Irvine et al., 2020, *Hydrol. Process.* The published version is available at: https://onlinelibrary.wiley.com/doi/abs/10.1002/hyp.13614

Quantitative guidance for efficient vertical flow measurements at the sediment-water interface using temperature-depth profiles

Running title

Quantitative guidance on the use of *T-z* methods

Authors

Dylan J. Irvine[1, *]

Barret L. Kurylyk[2]

Martin A. Briggs[3]

Affiliations

[1]College of Science and Engineering and National Centre for Groundwater Research and Training, Flinders University, Bedford Park, South Australia, 5042, Australia.

[2] Department of Civil and Resource Engineering and Centre for Water Resources Studies, Dalhousie University, Halifax, Nova Scotia, Canada

[3] U.S. Geological Survey, Earth System Processes Division, Hydrogeophysics Branch, Storrs, Connecticut, USA

* corresponding author, Dylan Irvine, dylan.irvine@flinders.edu.au, +61 8 8201 5730

Key words

Groundwater-surface water exchange	Analytical solutions
Groundwater discharge	Streambed mapping
Hyporheic flow	Gaining stream
Heat as a groundwater tracer	River-aquifer interactions

Graphic Abstract text

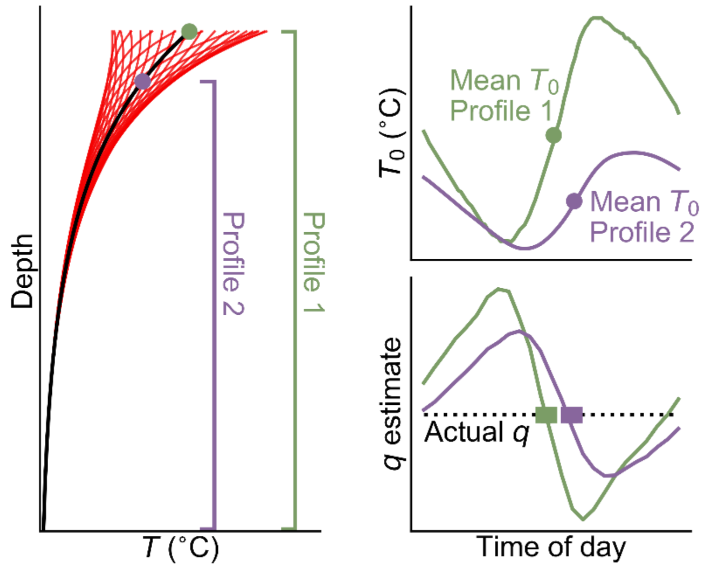

Steady-state temperature-depth (*T-z*) profile methods to quantify vertical surface water-groundwater exchange fluxes are influenced by diurnal temperature variations. We provide guidance to best apply these methods to obtain reliable flux estimates. We show that flux estimates are most accurate when the shallowest temperature profile measurement approximates its daily mean temperature. In some cases, flux estimates are improved by omitting the most transient (shallow) part of a *T-z* profile (see profile 2), or by using the daily mean of time series-based *T-z* profiles.

Abstract

Upward discharge to surface water bodies can be quantified using analytical models based on temperature-depth (*T-z*) profiles. The use of sediment *T-z* profiles is attractive as discharge estimates can be obtained using point-in-time data that are collected inexpensively and rapidly. Previous studies have identified that *T-z* methods can only be applied at times of the year when there is significant difference between the streambed-water interface and deeper sediment temperatures (e.g., winter and summer). However, surface water temperatures also vary diurnally, and the influence of these variations on discharge estimates from *T-z* methods is poorly understood. For this study, synthetic *T-z* profiles were generated numerically using measured streambed interface temperature data to assess the influence of diurnal temperature variations on discharge estimation and provide insight into the suitable application of *T-z* methods. Results show that the time of day of data collection can have a substantial influence on vertical flux estimates using *T-z* methods. For low groundwater discharge fluxes (e.g. 0.1 m d^{-1}), daily transience in streambed temperatures led to relatively large errors in estimated flow

magnitude and direction. For higher discharge fluxes (1.5 m d^{-1}), the influence of transient streambed temperatures on discharge estimates was strongly reduced. Discharge estimates from point-in-time *T-z* profiles were most accurate when the uppermost point in the *T-z* profile was near the bed interface daily mean (two time periods daily). Where temperature time series data are available, daily averaged *T-z* profiles can produce accurate discharge estimates across a wide range of discharge rates. Seasonality in shallow groundwater temperature generally had a negligible influence on vertical flow estimates. These findings can be used to plan field campaigns and provide guidance on the optimal application of *T-z* methods to quantify vertical groundwater discharge to surface water bodies.

1. Introduction

Groundwater discharge influences stream biogeochemistry (Boulton, Findlay, Marmonier, Stanley & Valett, 1998; Schmidt, Bayer-Raich & Schirmer, 2007; Caissie, Kurylyk, St-Hilaire, El-Jabi & MacQuarrie, 2014) and maintains steady and spatially diverse stream temperatures, providing thermal refugia for aquatic species (Brunke & Gonser 1997; Boulton et al., 1998; Anibas et al., 2009; Wondzell, 2011; McCobb, Briggs, LeBlanc, Day-Lewis & Johnson, 2018; Kurylyk, MacQuarrie, Linnansaari, Cunjak & Curry, 2015). Characterizing the vertical exchange of water between surface water bodies and groundwater (or vertical hyporheic return flow) can also be vital to determine the fate and transport of groundwater contaminants (Conant, 2004; Schornberg, Schmidt, Kalbus & Fleckenstein, 2010). However, most point-scale quantitative groundwater discharge measurement techniques are time and labor intensive (e.g. González-Pinzón et al., 2015). Time constraints often limit the scope of evaluations of groundwater-influenced habitat and reactive exchange. As the capabilities of large-scale numerical models of groundwater-surface water exchange continue to expand (e.g. Sulis et al., 2010), there is a critical need to implement efficient field measurement techniques across space and time to generate more appropriate validation and calibration data for such models.

Vertical water flow across the sediment-water interface can be measured directly using seepage meters (e.g. Lee, 1977; Murdoch & Kelly, 2003; Rosenberry, 2008), be inferred from Darcy's law using measured hydraulic gradients and estimates of hydraulic conductivity (Conant, 2004), or using geochemical techniques (e.g. Cranswick, Cook & Lamontagne, 2014). However, flowing water in streams and rivers can complicate the use of seepage meters even with design modification (Rosenberry, 2008), and the instruments are difficult to properly seal to armored streambeds. Estimates of upwelling based on Darcy's law are uncertain given the large range and spatially variable nature of sediment hydraulic conductivity (Calver, 2001; Cardenas & Zlotnik, 2003). Natural groundwater tracers offer an alternative approach to measure vertical flow rate. In particular, the use of heat as a tracer of groundwater discharge has increased in recent years, following reviews by Anderson (2005), Constantz (2008) and Rau, Andersen, McCallum, Roshan, and Acworth (2014). Heat tracer methods offer several advantages over chemical or hydraulic methods, primarily because temperature data can be measured inexpensively and easily, without laboratory analyses (Anderson, 2005; Anibas et al., 2009; Irvine et al. 2017a; Kurylyk, Irvine & Bense, 2019). Groundwater temperature data can often be collected using hydrogeology instruments (e.g. pressure transducers or conductivity loggers) already deployed on site for other purposes (Kurylyk & Irvine, 2019). Logging thermistors do not typically experience drift problems that plague other types of groundwater parameter data collection. Several open-source software packages are also available to automate thermal data analysis to estimate rates of groundwater-surface water exchange from temperature data using analytical or numerical methods (e.g. Gordon, Lautz, Briggs & McKenzie, 2012; Irvine, Lautz, Briggs, Gordon & McKenzie, 2015a; Koch et al. 2016; Kurylyk et al., 2017; Munz & Schmidt, 2017).

Temperature-based analytical solutions to quantify fluid exchange between surface water and groundwater fall into two categories: those based on the analysis of diurnal temperature signals (e.g. Hatch, Fisher, Revenaugh, Constantz & Ruehl, 2006, Keery, Binley, Crook & Smith, 2007; McCallum, Andersen, Rau & Acworth, 2012; Luce, Tonina, Gariglio & Applebee, 2013), and those that use 'steady-state' temperature depth (*T*-*z*) profiles (e.g. Bredehoeft & Papadopulos, 1965; Shan & Bodvarsson, 2004; Turcotte & Schubert, 2014). These methods differ in that the diurnal temperature signal-based methods use temperature time series at two or more depths, whereas *T*-*z* profile-based methods utilize point-in-time data at multiple depths.

The attributes of the diurnal temperature signal-based analytical solutions have been investigated broadly, including the influence of heterogeneity (Irvine, Cranswick, Simmons, Shannafield & Lautz, 2015b; Birkel et al. 2016), non-sinusoidal temperature signals (Luce, Tonina, Applebee & DeWeese, 2017), non-constant fluid fluxes (Irvine et al., 2015a, Rau, Cuthbert, McCallum, Halloran & Andersen, 2015), multi-dimensional flow (Lautz, 2010; Cuthbert & Mackay, 2013; Reeves & Hatch, 2016), and the uncertainty in flux estimates that results from uncertainties in thermal properties (Shanafield, Hatch & Pohll, 2011; Irvine et al., 2017a).

Steady-state, *T-z* methods have been utilized in a wide range of applications, including aquifer-scale estimates of vertical groundwater flow (Cartwright, 1970; Ferguson & Woodbury, 2003; Bense & Kooi, 2004; Irvine et al., 2017b; Kurylyk et al., 2017) and submarine groundwater discharge (Kurylyk et al., 2018; Tirado-Conde, Engesgaard, Karan, Muller & Duque, 2019). However, *T-z* methods are most widely used to estimate groundwater discharge to inland surface water bodies (e.g. Schmidt, Conant, Bayer-Raich & Schirmer, 2007; Anibas et al., 2009; Anibas, Buis, Verhoeven, Meire & Batelaan, 2011; Caissie et al., 2014; Kurylyk et al., 2017). For a detailed review on the use of *T-z* methods across a range of environments, the reader is directed to Kurylyk, Irvine and Bense (2019).

The use of *T-z* methods offers major advantages over diurnal temperature signal methods in that estimates of vertical water fluxes can be obtained using point-in-time or short-term (less than a full signal period) data. This allows rapid quantification of the spatial distribution of groundwater discharge to surface water bodies that is not possible with time-intensive diurnal temperature signal methods for which it is advised that data be collected for several consecutive days (Hatch, Fisher, Revenaugh, Constantz & Ruehl, 2006; Gordon, Lautz, McKenzie & Briggs, 2012).

There have also been several investigations into the implications of field conditions not meeting assumptions of the *T-z* methods. For example, large 2D spatial variations in hydraulic conductivities caused by streambed heterogeneity can lead to large errors in discharge estimates due to lateral conduction of heat (Schornberg, Schmidt, Kalbus & Fleckenstein, 2010; Ferguson & Bense, 2011). The role of annual temperature variations at the sediment-water interface is also important because steady state *T-z* methods rely on the curvature of a thermal profile to quantify flux; these methods perform poorly when there is little thermal difference between surface water and groundwater (i.e. a uniform *T-z* profile) (e.g. Schmidt et al., 2007; Schornberg et al., 2010; Anibas et al., 2011).

While the influence of annual temperature variation on the upper boundary condition has been investigated (e.g. Anibas et al., 2009), it is important to note that stream temperatures also typically vary diurnally. The influence of diurnal surface water temperature variations and superimposed annual temperature variation at the upper boundary on discharge estimates from *T-z* methods is currently poorly understood, limiting the uptake of this relatively efficient method for flux estimation. We postulate that certain characteristic times of day can be chosen for *T-z* data collection to enhance the likelihood of accurate vertical flux estimates, negating the need for data collection over time and thereby increasing practical spatial coverage. Thus, the aims of this study are to explore the optimal application of *T*-z methods to quantify vertical flow to surface water bodies. In particular, we 1) investigate the influence of diurnal temperature variations with and without superimposed annual temperature variations on discharge estimates from *T-z* methods, 2) explore the validity of utilizing daily mean *T-z* profiles where time series data are available, 3) investigate the implications of omitting the shallow portion of a *T-z* profile from analyses, and 4) utilize the above points to provide practical field deployment and data analysis guidance on the use of *T-z* methods to infer groundwater discharge to streams.

2. Methods

Details regarding the *T*-z methods theory, synthetic data creation, and data analysis are described in this section.

2.1 Heat transport theory

Following Bredehoeft and Papadopulos (1965), the equation for steady-state, one-dimensional (1D) subsurface heat transport with fluid flow can be written as:

$$\lambda_0 \frac{\partial^2 T}{\partial z^2} - qC_w \frac{\partial T}{\partial z} = 0, \qquad (1)$$

where λ_0 is the bulk thermal conductivity of the saturated sediment (W m^{-1} °C^{-1}), T is temperature (°C), z is sediment depth (m), q is the vertical fluid flux (positive downwards, m s^{-1}), and C_w is the volumetric heat capacity of the water (J m^{-3} °C^{-1}).

Bredehoeft and Papadopulos (1965) presented an analytical solution to Equation (1) as a method to determine q from *T-z* profiles:

$$T(z) = T_0 + (T_L - T_0)\frac{\exp(\beta z/L) - 1}{\exp(\beta) - 1}, \qquad (2)$$

where $T(z)$ is the temperature at depth, z, β is the dimensionless Peclet number calculated as ($\beta = C_w qL/\lambda_0$), T_0 and T_L are the temperatures at the top (i.e. z_0) and bottom (i.e. z_L) of the profile respectively (°C), and L is the length of the profile (m). If C_w and λ_0 are known and conditions are at steady-state, q can be determined by optimizing β to fit Eqn. 2 to an observed T-z profile. Here we define the inferred flux from this method as q_{BP}. The Bredehoeft and Papadopulos (1965) method (herein referred to as the BP method) was extended to allow for variations in thermal conductivity with depth for applications in the vadose zone (Shan & Bodvarsson, 2004) or saturated, layered sediments (Kurylyk et al., 2017); however, layered systems are not considered here.

Fundamentally, the BP method is based on the predicted departure of the T-z profile from a linear diffusive (conductive) thermal gradient to a thermal gradient with curvature produced by vertical fluid flow. The magnitude and directionality of the curvature (concave up or down) is directly related to λ_0 and q. A key benefit of the BP method is that only point-in-time data are required, thereby substantially reducing the effort required in data collection. Additional benefits include that the BP method only requires that two thermal properties, i.e. C_w which is essentially known (although variations due to temperature and/ or salinity occur), and λ_0. In contrast, methods that use diurnal temperature time series require data spanning several days. Also, the thermal properties required to determine discharge from diurnal time series include C_w, the volumetric heat capacity of the solids, C_s (J m^{-3} °C^{-1}), porosity (n), and λ_0 (e.g. Hatch, Fisher, Revenaugh, Constantz & Ruehl, 2006, Keery, Binley, Crook & Smith, 2007), or C_w, C_s and n (e.g. McCallum, Andersen, Rau & Acworth, 2012; Luce, Tonina, Gariglio & Applebee, 2013).

2.2 Synthetic data generation

Synthetic time-varying temperature fields were produced using the finite element groundwater flow and transport model FEFLOW (Diersch, 2014). The 1D numerical model domain used for most experiments was a saturated sediment column that was 4 m in the vertical direction, with a vertical discretization of 0.0125 m (Fig. 1). Later experiments investigate the influence of annual temperature signals. These simulations either used the 4 m model domain, or a 10 m high model, with a vertical discretization of 0.0125 m for the upper 2 m, ~0.02 m between 2 and 4 m, and ~0.03 m between 4 and 10 m.

Water flux through the models was varied using a specified flux boundary (constant in time). The upward fluxes tested in the model (denoted q_F) ranged from relatively low (-0.1 m d^{-1}) to high (-1.5 m d^{-1}). This range spans the fluxes either measured in field studies or used in other synthetic studies (e.g. Schmidt et al., 2007; Anibas et al., 2009; Anibas et al., 2011; Schornberg, Schmidt, Kalbus & Fleckenstein, 2010; Ferguson & Bense, 2011). The domain properties were $\lambda_0 = 2.5$ W m^{-1} °C^{-1}, $C_w = 4.18\times10^6$ J m^{-3} °C^{-1}, and C (bulk heat capacity of matrix) = 2.53×10^6 J m^{-3} °C^{-1}, which represent properties for saturated sand.

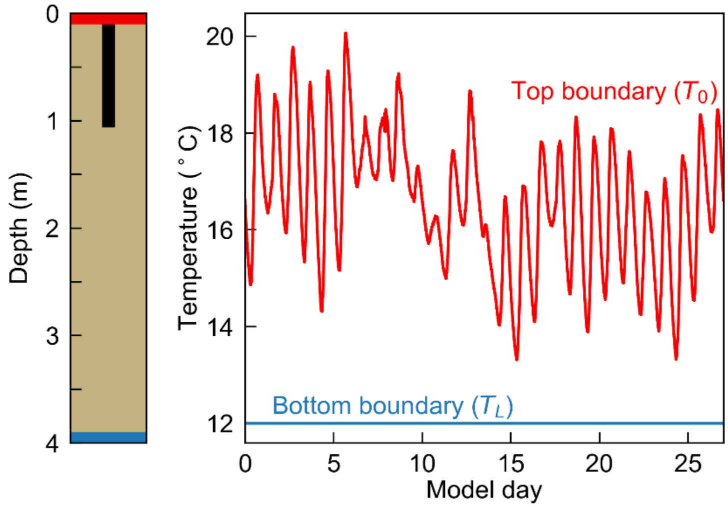

Figure 1: Numerical model set up (left) and temperature boundary conditions (right). *T-z* profiles were extracted from the upper 1 m of the model (black bar). Red data (right) are modified (detrended) from Zimmer and Lautz (2014) so that the temperatures at the first and last time steps were equal.

For all simulations, temperature time series were extracted at all nodes in the upper 1 m of the model domain as this represents a typical length of a sediment temperature probe. To more closely replicate the temperature resolution of commonly applied temperature loggers, the resolution of the modeled temperatures was set to 0.05 °C. This resolution falls between 0.02 °C of a HOBO Water Temp Pro v2 and 0.0625 °C of a Thermochron iButton.

2.2.1 Model set up for diurnal temperature signals

Temperature time series data from the field work of Zimmer and Lautz (2014) were used to specify the temperatures at the upper boundary (i.e. T_0, Fig. 1). These temperature time series were measured in the bed materials of Chittenango Creek, New York. The original dataset was detrended, so that the first and last temperature values were identical. A constant temperature of 12 °C was applied at the lower boundary (i.e. T_L) to represent local shallow groundwater temperature. The use of a constant temperature at 4 m depth was appropriate, given the short duration of the model simulations (27 days). The simulations were run twice, with the final temperature field from the first run used as the initial condition for the second. This approach removed the influence of the initial temperature conditions on the simulation.

2.2.2 Model set up for superimposed diurnal and annual signals

Simulations were also performed to investigate the role of annual temperature signals on the use of *T-z* methods. To generate annual temperature signals for the lower streambed boundary condition, the approach of Goto, Yamano and Kinoshita (2005) was used:

$$T(z,t)=\sum_i A\exp\left(\frac{v_{th}z}{2\kappa_e}-\frac{z}{2\kappa_e}\sqrt{\frac{\alpha+v_{th}^2}{2}}\right)\cos\left(\frac{2\pi t}{P}-\frac{z}{2\kappa_e}\sqrt{\frac{\alpha-v_{th}^2}{2}}\right), \tag{3}$$

where A is the annual amplitude (°C), v_{th} (i.e. $v_{th}=q\,C_w/C$) is the thermal front velocity (m s^{-1}), κ_e is thermal diffusivity (m^2 s^{-1}), P is the period (1 year), and α is defined as:

$$\alpha=\sqrt{v_{th}^2+\left(8\pi\kappa_e/P\right)^2}\ . \tag{4}$$

The lower boundary conditions were generated assuming a regional recharge rate of 100 mm y^{-1} (although the solution is relatively insensitive to this value). To produce the upper model boundary, an annual amplitude (A in Eq. 3) of the surface water (and hence the upper boundary, z_0) 8 °C was used (Fig. 2). The diurnal data from Zimmer and Lautz (2014) was superimposed on top of this annual signal to produce the upper boundary condition for the model.

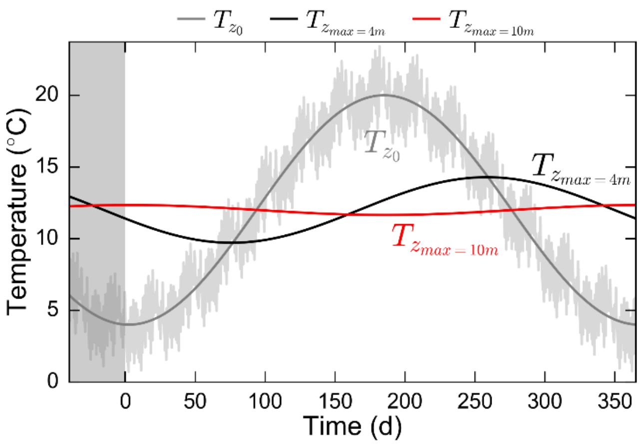

Figure 2: Temperatures for the upper boundary (grey), as well as T_L at 4 m (black) and 10 m (red). Grey zone denotes model spin up period.

Two simulations were considered to investigate the role of annual temperature signals at the lower boundary. The first of these used the regular 4 m high model domain (Fig. 1, left). The temperatures at the lower boundary (z = 4 m) were generated using Eqn. 3, with a z = 4 m, representing the maximum depth that nearby recharged water infiltrated to before discharging to the stream. We herein refer to this maximum depth as z_{max}. The second simulation used z_{max} = 10 m in Eqn. 3. This simulation used a larger model domain, applying this temperature time series at the model bottom (z = 10 m). Diurnal signals decay in the ~ 1m or so (Constantz, 2008), and thus diurnal signals were not included in the lower (4 m or 10 m depth) boundary. Initial conditions for the simulations to investigate the influence of annual temperature signals were produced using a steady state simulation with the first value from the generated time series as the boundary conditions. The transient simulations were run with 40 days of spin up time to remove the influence of the initial model conditions on the simulated temperatures.

2.3 Data analysis

The fitting of Eqn. 2 to field data can be readily automated by minimizing the difference between an observed and simulated *T-z* profile. While there are spreadsheet tools available for this (e.g. Arriaga & Leap, 2006; Kurylyk et al., 2017), the large number of *T-z* profiles requiring analysis here was better suited to a scripting environment. As such, q_{BP} values were estimated by minimizing the Root Mean Square Error (RMSE, °C) between the Bredehoeft and Papadopulos (1965) solution and the FEFLOW output using the Nelder and Mead (1965) minimization method in Python. Only β was adjusted in this optimization routine, as the thermal properties were known. The top and bottom boundaries were generally assigned from the temperatures at 0 and 1 m in the simulated profile, although the depth selection of the upper boundary was also explored (see Section 3.2).

Estimates of q_{BP} were produced using either point-in-time or daily averaged *T-z* profiles extracted from the modeled data set. The q_{BP} values were then compared to the known groundwater flux, q_F, from the FEFLOW simulations.

3. Results and Discussion

Sections 3.1 to 3.3 below use the temperature boundary conditions outlined in Fig. 1, whereas Section 3.4 uses the boundary conditions outlined in Fig. 2.

3.1 Use of point-in-time *T-z* profiles

The influence of a diurnally varying upper boundary condition on *T-z* profiles under discharge conditions is shown in Fig. 3. As the discharge rate increases (i.e. from Fig. 3a-c to Fig. 3g-i), the depth that the surface temperature signal propagates reduces. The expected penetration depth of a diurnal (sinusoidal) temperature signal could be determined using properties of the temperature signal, flux and sediment (Briggs et al., 2014). This approach could be used to estimate the thermal envelope depth.

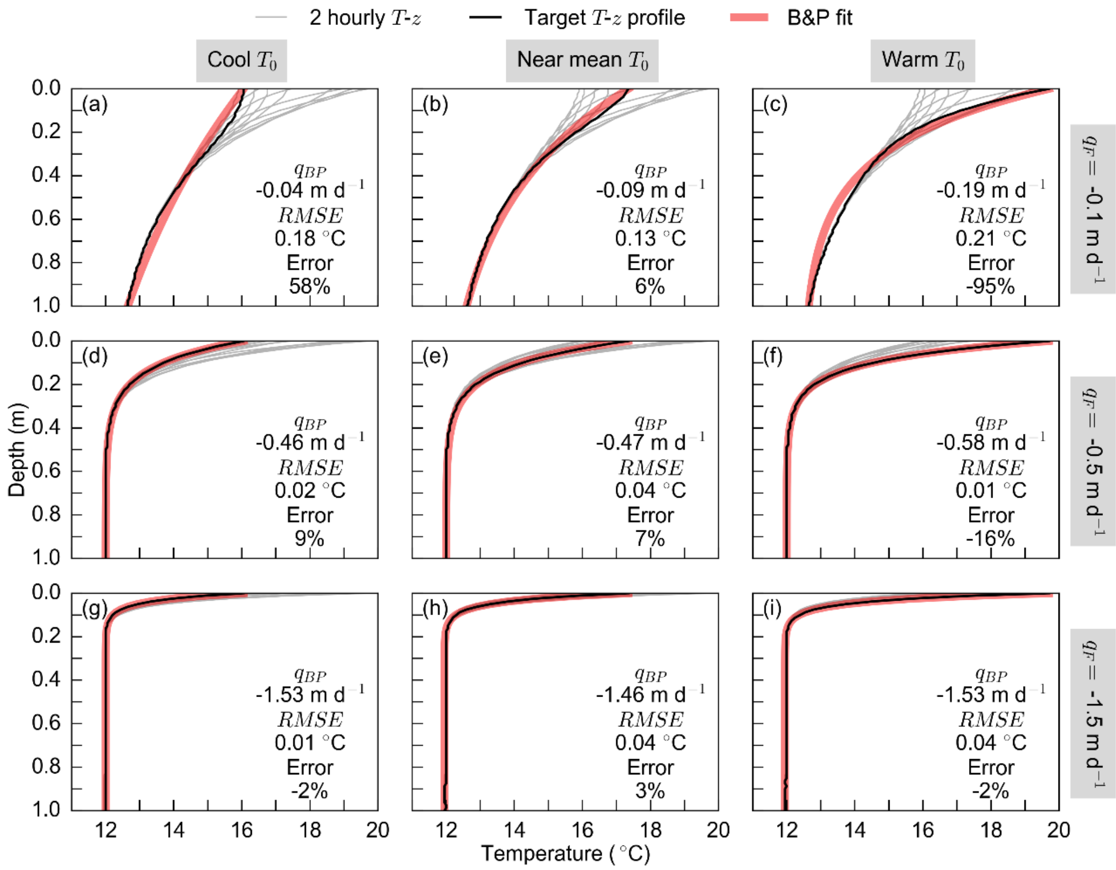

Figure 3: *T-z* profiles for q_F = -0.1 m d^{-1} (a, b, c), -0.5 m day^{-1} (d, e, f), and -1.5 m d^{-1} (g, h, i). Fitted BP solution (red) to simulated *T-z* profiles at different times of the day (black). Grey lines show two hourly *T-z* profiles throughout model day on the second day of the simulation. In each case, the root mean square error (RMSE, °C) between the synthetic and fitted *T-z* profiles is presented. Columns show fitted data where the surface temperature was cool (left, i.e. (a, d, g)), near the daily mean surface temperature (middle, i.e. (b, e, h)), and where the surface temperature was warm (right, i.e. (c, f, i)).

Fig. 3 shows *T-z* profiles that were extracted from the simulated temperature data in two-hour intervals, on the (arbitrarily selected) second day of the simulations. Using these *T-z* profiles, discharge was estimated at three times throughout the day: when T_0 was at its coolest (Figs 3a, d, g), when T_0 was near its daily mean (Figs. 3b, e, h), and at its daily maximum (Figs. 3c, f, i). In particular, the errors in estimated discharge are more pronounced for the q_F = -0.1 m d^{-1} case (top row), with flux magnitude under-estimates of 0.06 m d^{-1} (Fig. 3a) and over-estimates of 0.09 m d^{-1} (i.e., approaching 100% error, whereby negative errors denote stronger upwards flow, Fig. 1c), compared to the smaller errors for the q_F = -0.5 m d^{-1} case (Figs. 3d-f) and the q_F = -1.5 m d^{-1} case (Figs. 2g-i). Fig. 3 also suggests that the errors in the inferred flux are lowest when T_0 is at its mean; however, as the discharge rate increases, the importance of the timing of the T-z measurement decreases.

The presentation of the T-z profiles and fitted BP method in Fig. 3 only shows discharge estimates at three times across a 24-hour period (left, middle, right columns). However, when temperature time series data are available (as is the case here), it is possible to process T-z profiles at higher temporal resolution to further explore the role of transient boundary conditions on discharge estimates. Fig. 4 shows estimates of q_{BP} in 1-hour intervals for the low discharge case of q_F = -0.1 m d^{-1}. For a reference, the T_0 (from Fig. 1) is presented (Fig. 4a, black), as is the daily averaged mean temperature (Fig. 4a, red).

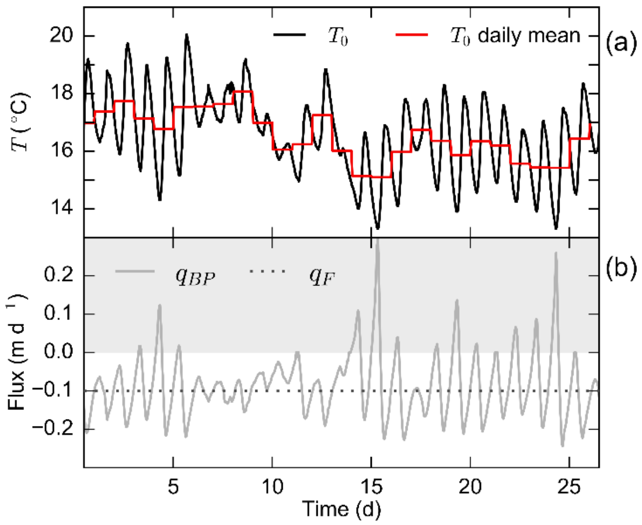

Figure 4: (a) T_0 (black) and the daily mean T_0 (red). (b) The calculated q_{BP} (grey) and the actual q_F = -0.1 m d^{-1} in FEFLOW (black dot). Any q_{BP} estimate in the shaded gray region has an incorrect flow direction.

The discharge estimates in Fig. 4b exhibit a diurnal pattern, generally oscillating around the known q_F value. As the true discharge flux was constant, the peaks and troughs of the periodic inferred flux time series represent the maximum errors in the inferred flux. These errors arise because the BP method attributes T-z profile curvature entirely to heat advection from groundwater flow, but profile curvature in these cases arises in large part from the diurnal transience. Errors in discharge estimates were relatively low (compared to other time periods) between model days six and 10 (errors on the order of ±0.05 m d^{-1}, Figure 4b). These errors are lower than the errors in other periods in the simulation because the T_0 diurnal amplitudes are also low during this time period, and thus the conditions more closely satisfy the steady-state assumptions of the BP method. Time periods with low amplitudes of the diurnal temperature signals pose challenges when applying diurnal temperature signal methods. The use of the BP method may be able to supplement time periods where diurnal signal-based flux estimates are deemed to be unreliable.

The temperature change (Fig. 4a) at this low discharge flux can cause even the direction of the inferred flux to be in error (Fig. 4b). For example, the q_{BP} estimate of 0.30 m d^{-1} (near day 15, Fig. 4b) represents an error on the order of 400%. In general, positive (downwards) estimates of q_{BP} should be perceived with caution as *T-z* methods are generally not used to estimate downwards flow (e.g. Schmidt et al., 2007) unless the upper boundary temperatures are relatively constant. For example, downwards flow (i.e. groundwater recharge) has been determined using the BP method in streams that experience seasonal ice cover (e.g. Caissie et al., 2014), or in deep-ocean seafloor sediments (Kurylyk et al., 2018).

The data analysis procedure shown in Fig. 4 is repeated in Fig. 5, where the results of the analyses of the q_F = -1.0 m d^{-1} case are shown. While the q_F estimates in Fig. 5b have the same oscillatory behavior as was the case where q_F = -0.1 m d^{-1} (Fig. 4b), it is important to note that the q_{BP} estimates are generally more accurate (i.e. the signal amplitude/mean ratio is much lower). For example, the q_{BP} estimates generally fall within ±0.1 m d^{-1}, representing errors on the order of ±10%, far below, for example, the uncertainty of fluxes estimated from head data via Darcy's Law.

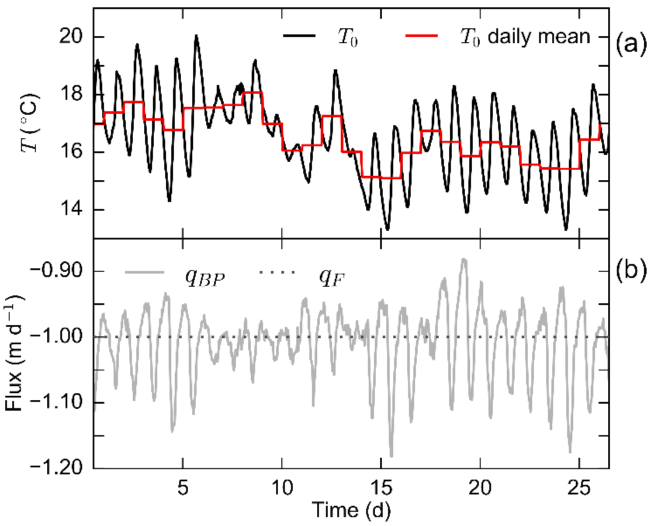

Figure 5: (a) T_0 (black) and the daily mean T_0 (red). (b) The calculated q_{BP} (grey) and the actual q_F = -1.0 m d^{-1} in FEFLOW (black dot).

In both Figs 4b and 5b, the q_{BP} estimates are most accurate as the T_0 signals approach the daily mean temperature ($\bar{T}_0$). This finding could be particularly useful if a dense network of discharge estimates is to be collected within a short period of time. For example, Schmidt et al. (2007) used a dense network of *T-z* profiles to produce spatial maps of discharge for the Pine River in Ontario, Canada. The fact that the first occurrence of the mean daily surface water temperature typically occurs mid-late morning is particularly useful given that daily field campaigns are often launched around this time.

To further explore the impact of the intra-daily timing of the collection of field *T-z* profiles, errors in discharge estimates are presented against the difference between a point-in-time T_0, and the $\bar{T}_0$ for a range of discharge rates (Fig. 6).

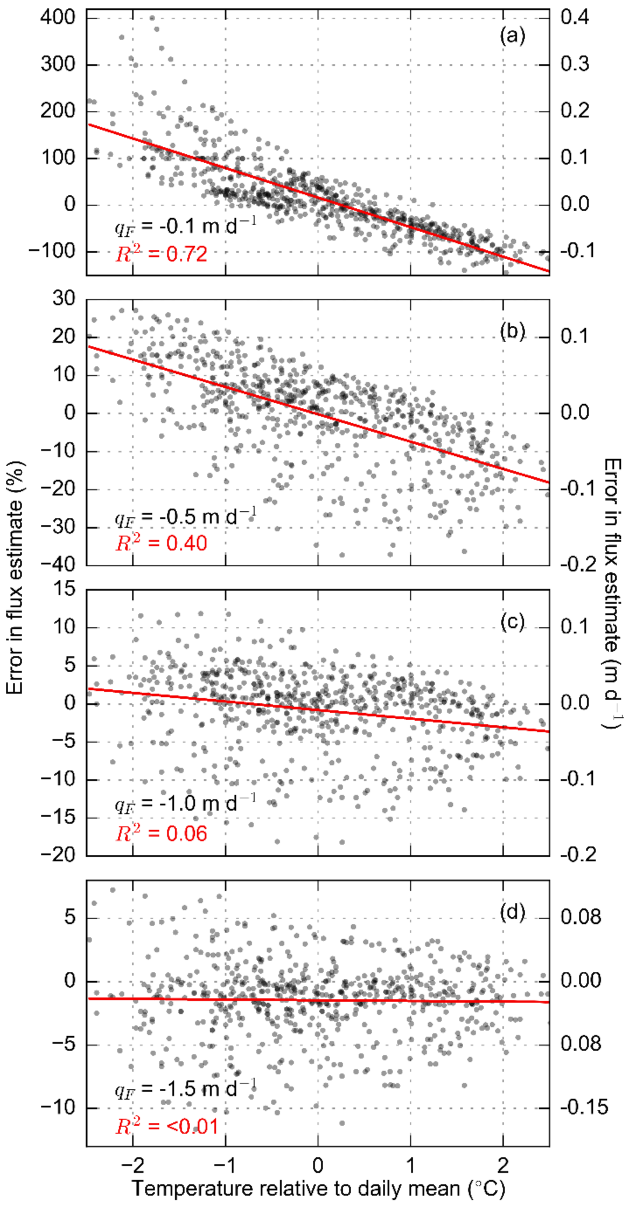

Figure 6: Errors in flux estimates (in %, left axis, and m d^{-1}, right axis) against the temperature difference between T_0 and $\overline{T}_0$ (i.e. difference between black and red lines in Fig 4a, 5a) for q_F = -0.1 m d^{-1} (a), -0.5 m d^{-1} (b), -1.0 m d^{-1} (c) and -1.5 m d^{-1} (d). Red lines denote linear regression, with R^2 listed in red text. Note the changes in the left vertical scales from (a) to (d). Positive errors denote discharge estimates which are closer to zero, i.e. lower discharge rates. Negative errors denote stronger discharge.

In particular, the q_F = -0.1 m d^{-1} case (Fig. 6a) demonstrates for low discharge conditions, collection time of *T-z* profiles can significantly influence errors in q_{BP}. When T_0 was cooler than $\overline{T}_0$, discharge estimates yielded lower magnitudes, or suggested recharge conditions. For higher discharge rates (i.e. as shown in Figs. 6b-d), the regression slope decreases, as does the

R^2; highlighting that the importance of *T-z* profile collection time decreases with increasing flux. Also, the relative errors in q_{BP} estimates reduce substantially for higher discharge rates. For example, errors are generally within ±10% for q_{BP} = -1.5 m d^{-1} (Fig. 6d).

Discharge estimates (Figs. 3-6) are partly based on the highly transient shallow portion of the *T-z* profile. Previous work proposed transient thermal effects are minimized by omitting the shallow profile and/or reducing time series data down to a daily mean profile (Kurylyk et al., 2017); however, this approach has not been validated. Section 3.2 explores implication of omitting the shallow, transient portion of *T-z* profiles on vertical flux estimates. Section 3.3 considers the impact of analyzing daily mean *T-z* profiles and uncertainty in thermal properties.

3.2. Omitting the shallow, transient portion of the *T-z* profile

To consider the potential advantages of focusing on less transient portions of a *T-z* profile, we consider profiles with the top boundary imposed at different depths below the stream-sediment interface. The results in Fig. 7 show the estimated q_{BP} values for q_F = -0.1 m d^{-1} (Fig. 7a, b), and q_F = -0.5 m d^{-1} (Fig. 7c, d). In both cases, three lengths of the *T-z* profiles were used to determine q_{BP}. Profiles sections were selected in which the entire profile was used (upper depth, z_0, = 0 m), and in which the upper 0.1 and 0.2 m of the profile were excluded from the analyses (i.e. z_0 occurs at depths of 0.1 and 0.2 m).

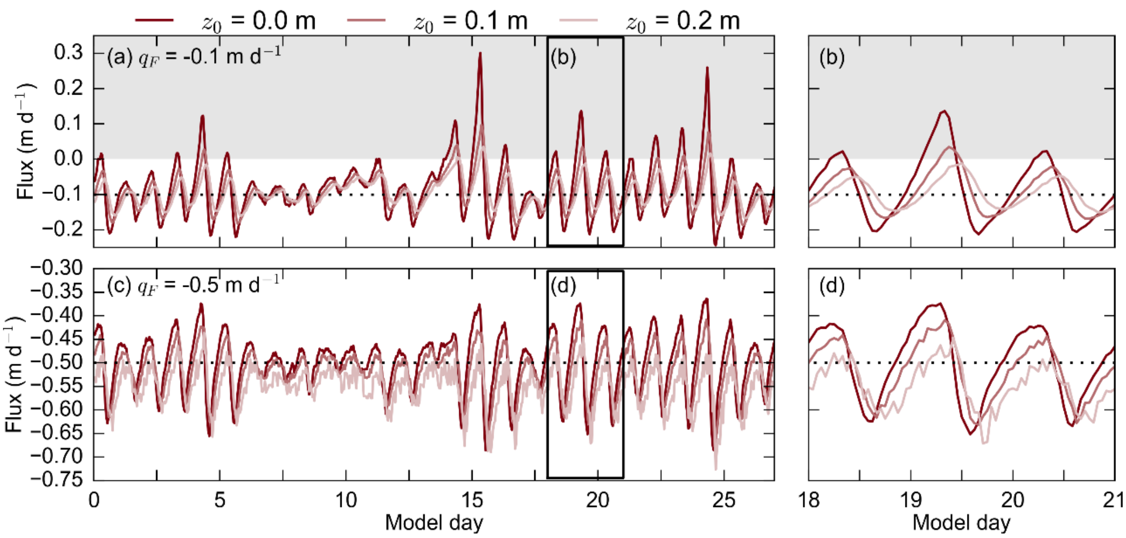

Figure 7: Discharge estimates using point-in-time data. Estimates produced using *T-z* profiles between the upper depth of the profile, z_0 (m), and 1 m in depth (see legend). Results shown for (a) q_F = -0.1 m d^{-1}, with subset shown in (b), and (c) q_F = -0.5 m d^{-1} with subset shown in

(d). Grey shading in (a-b) denotes where the flow direction of q_{BP} is incorrect. The known q_F is shown in dotted black.

For the q_F = -0.1 m d^{-1} case (Fig. 7a, b), the discharge estimates became increasingly accurate (amplitudes in inferred q_F time series decrease) as the upper, most thermally transient portion of the *T-z* profile was omitted from the analyses. The diurnal nature of the q_{BP} estimates has a phase lag as the z_0 increases (Figure 7a, b). This effect is related to the timing of the propagation of the surface signal to the uppermost temperature measurement used in the *T-z* profile. Thus, errors in estimation of vertical fluxes from the BP method will typically be lower when the temperature used for the upper boundary condition (T_0 at depth z_0) is near its daily mean.

The reduction in error with the use of an increasingly deeper z_0 as shown in Figs. 7a-b is not universally replicated for the q_F = -0.5 m d^{-1} case (Fig. 7c, d). Figs. 7c-d visually shows that errors reduce when z_0 = 0.1 m, but that discharge rates are then generally over-estimated (i.e. q_{BP} are more highly negative) where z_0 = 0.2 m. Tabulated statistics of errors (max-over and max-under estimates, means and standard deviations) for several discharge scenarios are presented in Table 1 below. The data presented in Table 1 range from q_F = -0.1 to -1.0 m d^{-1}. Higher discharge results (i.e. -1.5 m d^{-1}) are not presented, as the shallow part of a *T-z* profile contains the useful information for flux estimation using the BP method under strong discharge conditions as discussed below.

Table 1: Errors in discharge estimates from point-in-time *T-z* profiles from z_0 to 1.0 m over the 27-day period of the model simulations. A negative error denotes stronger discharge than reality, positive errors denote weaker discharge.

		Error (m d^{-1})			
q_F (m d^{-1})	z_0 (m)	Max Over-estimate	Max Under-estimate	Mean	Standard deviation (σ)
-0.1	0.0	-0.144	0.401 †	0.015	0.082
-0.1	0.1	-0.090	0.197 †	0.007	0.053
-0.1	0.2	-0.067	0.136 †	0.005	0.039
-0.2	0.0	-0.144	0.181	0.007	0.059
-0.2	0.1	-0.084	0.120	0.005	0.042
-0.2	0.2	-0.062	0.100	0.004	0.031
-0.3	0.0	-0.169	0.158	0.004	0.060
-0.3	0.1	-0.114	0.108	0.001	0.044
-0.3	0.2	-0.090	0.082	-0.003	0.033

-0.4	0.0	-0.181	0.148	0.001	0.062
-0.4	0.1	-0.138	0.106	-0.008	0.047
-0.4	0.2	-0.135	0.065	-0.024	0.038
-0.5	0.0	-0.186	0.136	-0.001	0.063
-0.5	0.1	-0.178	0.091	-0.016	0.050
-0.5	0.2	-0.226	0.064	-0.051	0.043
-1.0	0.0	-0.182	0.119	-0.008	0.052
-1.0	0.1	-0.611	0.401	-0.078	0.124
-1.0	0.2	-153.075 ‡	1.196 †	-10.646	37.979

† denotes incorrect flux direction., ‡ denotes unrealistically large error due to very small difference between temperatures at z_0 and z_L

To explain why errors do not always decrease as the uppermost transient part of a *T-z* profile is omitted from the analysis, we explore the behavior of *T-z* profiles under idealized conditions using Eqn. 2. (i.e. with 1D flow and steady T_0). As discharge increases, the deeper portion of the *T-z* profile becomes vertical (uniform, e.g. see Figs. 3d-i). Thus, the shallow portion of a *T-z* profile contains the most useful information to determine discharge in the case of high fluxes. Fig. 8a shows the depth at which the vertical portion of a *T-z* profile will be reached, for various values of thermal conductivity and discharge rate. Fig. 8b shows four example *T-z* profiles to highlight the importance of the shallow data.

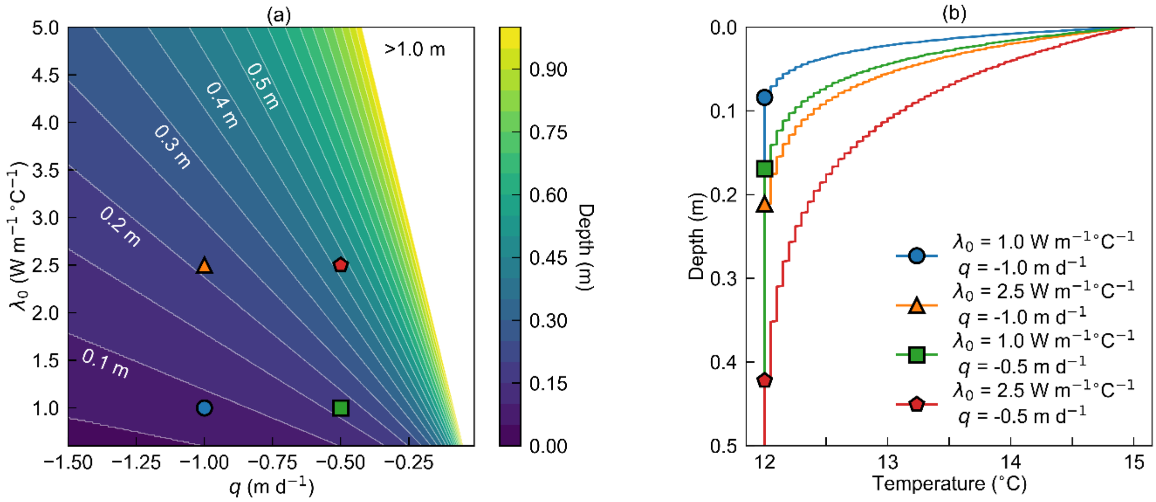

Figure 8: (a) The shallowest depth at which uniform temperatures are realized using Eq. 2. As the upwelling rate increases, or as thermal conductivity decreases, uniform temperatures are reached at shallower depths. Results shown for a temperature resolution of 0.05°C. Calculated depth of >1.0 m are shown in white. *T-z* profiles in (b) correspond to the markers in (a).

For conditions where q_F = -1.0 m d^{-1} and λ_0 =2.5 W m^{-1} °C^{-1} (Fig. 8, orange lines, triangle markers), the non-vertical portion of the *T-z* profile is restricted to the upper ~0.2 m of the profile. This explains why errors do not reduce as the shallow data are omitted from analyses in Figs. 6c-d but also highlights the importance of capturing data in the upper ~0.2 m of the bed materials. That is, removing this upper portion of the *T-z* profile removes the portion of the profile that may contain useful information to determine the vertical flux. Fig. 8 can provide insights into field data collection approaches if approximate thermal properties and an expected range of discharge rates are known.

The analyses presented in Figs. 7, 8 and Table 1 suggest that omitting the most transient portion of the *T-z* profile can reduce errors at low flux. However, the benefits of this approach are reduced as the discharge rate increases because the zone of useful temperature information for flux estimation collapses upward toward the water-bed interface. The portion of a *T-z* profile that contains useful information could be identified using the 'extinction depth' equation from Briggs et al. (2014). This approach is used to identify the maximum sediment depth for sinusoidal (i.e. diurnal) temperature signal-based analyses under varied flux conditions (e.g. Irvine et al. 2017a) but could also be applied to estimate the shallow portion of a *T-z* profile with greatest curvature for steady-state analyses. Fig. 8 highlights the fact that the thermal properties of the system should also be taken into consideration. In general, we recommend collecting the profile from the sediment surface downwards and then evaluating if the upper portion should be removed during data analysis based on whether the profile becomes vertical at shallow depths or not.

3.3 Use of daily averaged *T-z* profiles and uncertainties in thermal conductivity

When temperature time series data are available, the use of daily averaged *T-z* profiles can be another approach to reduce the influence of diurnal temperature variations at the upper boundary. This approach may be useful when a temperature profiler was installed for insufficient duration of time to apply diurnal temperature signal methods (e.g. Hatch, Fisher, Revenaugh, Constantz & Ruehl, 2006; McCallum, Andersen, Rau & Acworth, 2012), which typically benefit from omission of the first and last few days of the data set due to issues introduced by signal processing (Hatch, Fisher, Revenaugh, Constantz & Ruehl, 2006; Irvine et al., 2017a). A comparison of discharge fluxes inferred via the BP method for hourly *T-z* profiles (light shades) and daily averaged *T-z* profiles (darker shades, with markers) is shown in Fig. 9.

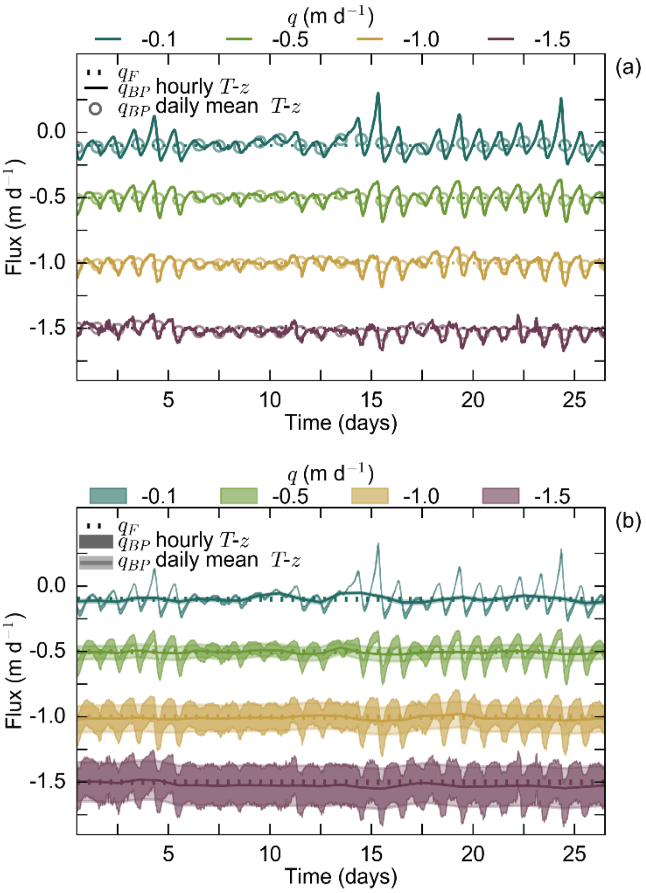

Figure 9: (a) q_{BP} estimates for q_F = -0.1, -0.5, -1.0 and -1.5 m d^{-1}. Darker shading denotes the q_{BP} estimates from hourly *T-z*. Lighter shade shows the q_{BP} estimates using daily mean *T-z* profiles. q_F for the cases shown here are denoted by the dotted line. (b) repeats the analyses in (a) but includes ±10% uncertainty in λ_0.

In particular, the reduction in error for the q_F = -0.1 m d^{-1} is significant when using daily averaged instead of point in time *T-z* profiles (Fig. 9a), with a maximum over-estimate of 0.048 m d^{-1} (48%), and maximum under-estimate of 0.030 m d^{-1} (30%) with the daily averaged approach. This error range does not exceed the uncertainty associated with fluxes estimated from head data. In contrast, the hourly *T-z* data produced discharge estimates with errors ranging from maximum under-estimates of 0.401 m d^{-1} (~400%) and maximum over-estimates of -0.144 m d^{-1} (~140%). While the benefits of the use of daily average *T-z* profiles diminishes as the discharge rate increases, in all cases considered, the use of daily average *T-z* profiles leads to more accurate discharge estimates.

The analyses considered thus far have assumed that thermal conductivity was known. With the form of Eqn. 2, the errors introduced to discharge estimates from unknown or poorly constrained thermal conductivities will be linear. For example, Fig. 9b repeats the analyses presented in Fig. 9a if λ_0 was known to ±10%. Even in cases where λ_0 has been measured, uncertainties will remain. For example, a Tempos Thermal Property Analyzer can measure λ_0 with an accuracy of ±10%. It is important to note that, if the material type is known, thermal conductivity can generally be reasonably well constrained from tabulated values of thermal conductivities (e.g. Stonestrom & Blasch, 2003; Anderson, 2005; Irvine et al., 2017a).

As a way of comparison between vertical fluxes estimated from point-in-time and daily averaged *T-z* profiles, maximum over- and under-estimates, as well as mean and standard deviations of q_{BP} estimates, are provided in Table 2.

Table 2: Errors in discharge estimates using point-in-time (PIT) or daily averaged (avg) *T-z* profiles. Negative error (in m d^{-1} or %) denotes estimates of stronger discharge that actual.

		Max over-estimate		**Max under-estimate**		**Mean error**		**Standard deviation (σ)**	
q_F (m d^{-1})	**Approach**	**m d^{-1}**	**%**	**m d^{-1}**	**%**	**m d^{-1}**	**%**	**m d^{-1}**	**%**
-0.10	PIT	-0.144	-144	0.401	401	0.015	15	0.082	82
-0.10	avg	-0.030	-30	0.048	48	0.002	2	0.023	23
-0.20	PIT	-0.144	-72	0.181	91	0.007	4	0.059	30
-0.20	avg	-0.021	-11	0.036	18	0.002	1	0.015	8
-0.30	PIT	-0.169	-56	0.158	53	0.004	1	0.060	20
-0.30	avg	-0.023	-8	0.037	12	0.000	0	0.014	5
-0.40	PIT	-0.181	-45	0.147	37	0.001	0	0.062	16
-0.40	avg	-0.023	-6	0.033	8	-0.004	-1	0.013	3
-0.50	PIT	-0.186	-37	0.136	27	-0.001	0	0.063	13
-0.50	avg	-0.023	-5	0.029	6	-0.006	-1	0.012	2
-0.75	PIT	-0.190	-25	0.140	19	-0.005	-1	0.059	8
-0.75	avg	-0.027	-4	0.017	2	-0.008	-1	0.011	1
-1.00	PIT	-0.182	-18	0.119	12	-0.008	-1	0.052	5
-1.00	avg	-0.032	-3	0.021	2	-0.010	-1	0.013	1
-1.25	PIT	-0.110	-9	0.135	11	0.021	2	0.045	4
-1.25	avg	-0.022	-2	0.030	2	0.018	1	0.010	1
-1.50	PIT	-0.174	-12	0.109	7	-0.022	-1	0.046	3
-1.50	avg	-0.050	-3	0.018	1	-0.022	-1	0.017	1

3.4 Investigating the influence of annual temperature signals

The results in Fig. 10 show that the addition of annual temperature signals, both at the upper and lower boundaries does not significantly alter the q_{BP} estimates for most of the year where there is a large difference between z_0 and z_L. The smaller oscillating errors (Fig. 10 d-f) are caused by the diurnal signals included in the boundary condition, while the large error spikes are introduced by the annual signals.

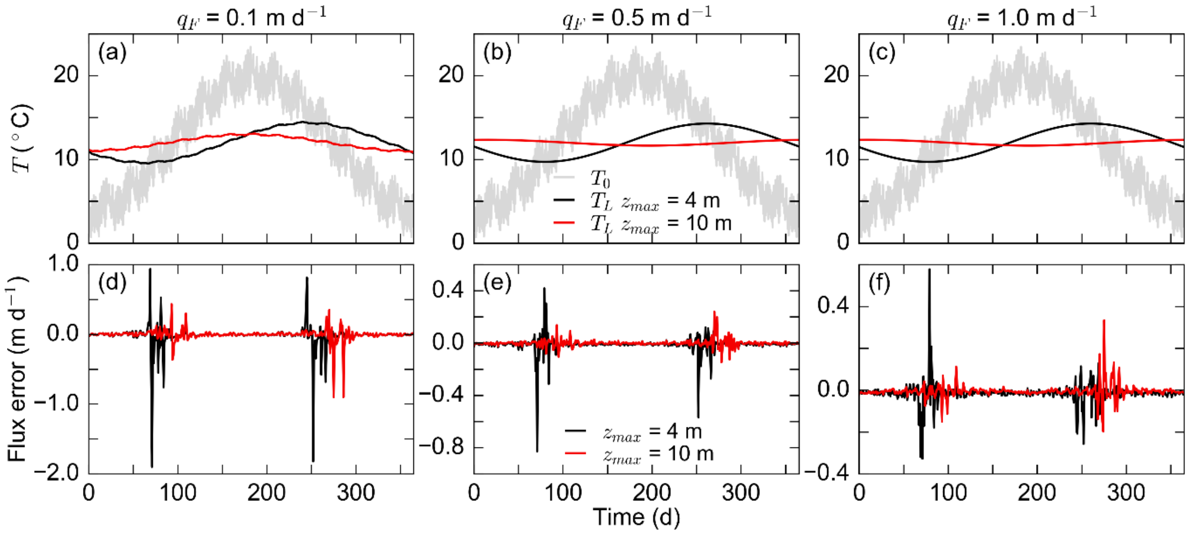

Figure 10: (a-c) Showing temperature time series used for the upper boundary (i.e. z_0, grey, superimposed diurnal and annual signals) and at z = 1 m for the z_{max} = 4 m simulation (black) and the z_{max} = 10 m simulation (red). (d-e) Errors in q_{BP} estimates using daily averaged T-z profiles. Note that the q_{BP} was removed for day 275 from the z_{max} = 10 m model results given that the T-z profile was near vertical and produced an unrealistically high error.

The errors for the z_{max} = 4 m models (Fig. 10d-f, black) were generally larger than the z_{max} = 10 m model (Fig. 10d-f, red). For example, the over- and under-estimates for the q_F = -0.5 m d^{-1} case (Fig. 10e) for the z_{max} = 4 m model ranged between -0.827 m d^{-1} and 0.419 m d^{-1} (mean -0.010 m d^{-1}). In comparison, the z_{max} = 10 m model errors ranged between -0.146 m d^{-1} and 0.240 m d^{-1} (mean ~0.0002 m d^{-1}). The largest over- and under-estimates occur during time periods where T_0 approaches T_L. These findings are generally consistent with the results of Anibas et al. (2009) and suggest that (1) annual and diurnal temperature signals are convoluted in shallow streambeds, but diurnal signals tend to overwhelm effects from annual signals and (2) when using T-z profile-based methods, it is typically more important to consider potential transient effects from diurnal signals than those from annual signals, except for periods in the year when there is no streambed thermal gradient. This finding is also applicable to the use of T-z profile-based methods for the quantification of shallow groundwater discharge rates, as groundwater with effective source flow path depth within approximately 6 m of land surface will commonly show a pronounced annual temperature signal (Constantz, 2008; Briggs et al. 2018)

4. Conclusions and implications for field studies

The cases considered here were for steady, uniform 1D flow under upwelling conditions. Groundwater discharge is typically most vertical toward the center of the stream channel, but becomes highly oblique toward the banks (Modica, 1999). Irvine, Cartwright, Post, Simmons and Banks (2016) highlighted that in multi-dimensional flow fields, *T-z* profile analyses provide an estimate of the average vertical flux over the length of the *T-z* profile. Thus, with multi-dimensional flows, varying the length of the *T-z* profile used may lead to discharge estimates over different lengths. In low discharge conditions, provided that sufficient density of data points are available along a profile, it may be possible to produce depth-dependent estimates of vertical fluxes.

The use of *T-z* profiles to provide point estimates of groundwater discharge is a promising technique, given that high-resolution temperature probes are relatively inexpensive, and that data can be collected rapidly, allowing spatial mapping of vertical fluxes that is otherwise difficult to achieve. Herein, we provide the first study and guidelines for considering and correcting for the impacts of diurnal temperature variability when assuming steady-state *T-z* profiles (i.e. Eqn. 2). We also consider the convolution of annual and diurnal temperature signals and their combined transient impacts on flux estimates derived from steady-state approaches. While data analyses are relatively straightforward, several steps in data collection and analysis can be taken to increase the likelihood of accurate discharge estimates:

(1) In cases where only point-in-time data are available, more accurate discharge estimates can be obtained when the upper *T-z* profile boundary is near its daily mean temperature. The importance of the timing of data collection decreases as the vertical flux increases.

(2) For lower-flux systems with strong surface diurnal temperature signals, it may be desirable to remove the shallowest section of *T-z* data from vertical flux analysis. The thickness of the removed section can be estimated using the predicted extinction depth of a diurnal signal amplitude. The omission of highly transient shallow temperature data is helpful in improving accuracy of vertical flux estimates for lower fluxes, but omitting the shallow data can be

problematic at high rates of upwelling (e.g. q < -0.5 m d^{-1}) as thermally uniform profiles develop at depth. It is beneficial to ensure that a thermal probe is used with many measurements of temperature (i.e. thermal sensors) available with depth to allow maximum flexibility for data analyses.

(3) If temperature time series data are available, accurate discharge estimates can be obtained by averaging (mean) the temperature data over a daily time period at each depth. This approach may be useful in cases where time series data are available but do not extend over a sufficient duration to apply diurnal temperature signal methods, or when diurnal signals are not ideally-formed such that the phase and amplitude cannot be accurately extracted.

(4) The propagation of annual temperature signals into shallow streambeds can create thermally uniform conditions with depth, making it challenging to apply thermal tracing approaches based on a *T-z* profile curvature (Anibas et al., 2009). These conditions can be checked at the beginning of a field campaign to prevent later data analysis issues.

In summary, spatially dense streambed upwelling mapping is possible using point-in-time profiles that can be efficiently recorded and analyzed using steady-state analytical approaches. Hydrologists have understood that these techniques have inherent limitations because streambeds exhibit diurnal thermal transience. Accordingly, they have employed more intensive methods based on diurnal thermal signal transfer. These methods require probes in place for multiple days of thermal data and thus limit the number of locations studied. Here we demonstrate that diurnal transience errors are minimal for strong upwelling, and can be minimized using the approaches above in the case of weak upwelling. In particular, judiciously selecting the time of day for data collection and the appropriate probe thermal sensor depths can reduce errors to values less than or comparable to those associated with most alternative techniques for quantifying upwelling.

Acknowledgements

Funding for this methods development was provided in part by U.S. Department of Energy grant DE-SC0016412 and the U.S. Geological Survey Toxic Substances Hydrology Program. Any use of trade, firm, or product names is for descriptive purposes only and does not imply endorsement by the U.S. Government. We declare no conflicts of interest. We would like to thank Mark Harvey and the two anonymous reviewers for their helpful reviews.

Data availability statement

The data that support the findings of this study are available from the corresponding author upon reasonable request.

References

Anderson MP. 2005. Heat as a ground water tracer. *Groundwater, **43***: pp. 951-968. DOI: 10.1111/j.1745-6584.2005.00052.x.

Anibas C, Fleckenstein JH, Volze N, Buis K, Verhoeven R, Meire P, & Batelaan O. 2009. Transient or steady-state? Using vertical temperature profiles to quantify groundwater-surface water exchange. *Hydrological Processes, **23***: pp. 2165-2177. DOI: 10.1002/hyp.7289.

Anibas C, Buis K, Verhoeven R, Meire P, & Batelaan O. 2011. A simple thermal mapping method for seasonal spatial patterns of groundwater-surface water interaction. *Journal of Hydrology, **397***: pp. 93-104. DOI: 10.1016/j.jhydrol.2010.11.036.

Arriaga MA, & Leap DI. 2006. Using solver to determine vertical groundwater velocities by temperature variations. *Hydrogeology Journal, **14***: pp. 253-263. DOI: 10.1007/s10040-004-0381-x.

Bense VF, Kooi H. 2004. Temporal and spatial variations of shallow subsurface temperature as a record of lateral variations in groundwater flow. J. Geophys. Res., **109**: B04103. DOI: 10.1029/2003JB002782.

Birkel C, Soulsby C, Irvine DJ, Malcolm I, Lautz LK, & Tetzlaff D. 2016. Heat-based hyporheic flux calculations in heterogeneous salmon spawning gravels. *Aquatic Sciences, **78***: pp. 203-213. DOI: 10.1007/s00027-015-0417-4.

Boulton AJ, Findlay S, Marmonier P, Stanley EH, & Valett HM. 1998. The functional significance of the hyporheic zone in streams and rivers. *Annual Review of Ecology and Systematics, **29***: pp. 59-81. DOI: 10.1146/annurev.ecolsys.29.1.59.

Bredehoeft JD, & Papadopulos IJ. 1965. Rates of vertical groundwater movement estimated from the Earth's thermal profile. *Water Resources Research, **1***: pp. 325-328.

Briggs MA, Lautz LK, Buckley SF, & Lane JW. 2014. Practical limitations on the use of diurnal temperature signals to quantify groundwater upwelling. *Journal of Hydrology, **519***: pp. 1739-1751. DOI: 10.1016/j.jhydrol.2014.09.030.

Briggs MA, Johnson ZC, Snyder CD, Hitt NP, Kurylyk BL, Lautz L, Irvine DJ, Hurley ST, Lane JW. 2018. Inferring watershed hydraulics and cold-water habitat persistence using multi-year air and stream temperature signals. *Science of the Total Environment*, **636**: 1117-1127. DOI: 10.1016/j.scitotenv.2018.04.344.

Brunke M, & Gonser T. 1997. The ecological significance of exchange processes between rivers and groundwater. *Freshwater Biology, **37***: pp. 1-33. DOI: 10.1046/j.1365-2427.1997.00143.x.

Caissie D, Kurylyk BL, St-Hilaire A, El-Jabi N, & MacQuarrie KTB. 2014. Streambed temperature dynamics and corresponding heat fluxes in small streams experiencing seasonal ice cover. *Journal of Hydrology, **519***: pp. 1441-1452. DOI: 10.1016/j.jhydrol.2014.09.034.

Calver A. 2001. Riverbed permeabilities: Information from pooled data. *Groundwater, **39***: pp. 546-553. DOI: 10.1111/j.1745-6584.2001.tb02343.x.

Cardenas MB, & Zlotnik VA. 2003. Three-dimensional model of modern channel bend deposits. *Water Resources Research, **39***. DOI: 10.1029/2002wr001383.

Cartwright K. 1970. Groundwater discharge in the Illinois Basin as suggested by temperature anomalies. *Water Resources Research, **6***: pp. 912-918.

Conant B. 2004. Delineating and quantifying ground water discharge zones using streambed temperatures. *Groundwater, **42***: pp. 243-257. DOI: 10.1111/j.1745-6584.2004.tb02671.x.

Constantz J. 2008. Heat as a tracer to determine streambed water exchanges. *Water Resources Research, **44***. DOI: 10.1029/2008wr006996.

Cranswick RH, Cook PG, & Lamontagne S. 2014. Hyporheic zone exchange fluxes and residence times inferred from riverbed temperature and radon data. *Journal of Hydrology, **519***: pp. 1870-1881. DOI: 10.1016/j.jhydrol.2014.09.059.

Cuthbert MO, & MacKay R. 2013. Impacts of nonuniform flow on estimates of vertical streambed flux. *Water Resources Research, **49***: pp. 19-28. DOI: 10.1029/2011wr011587.

Diersch H-JG. 2014. FEFLOW: Finite Element Modeling of Flow, Mass and Heat Transport in Porous and Fractured Media. Springer.

Ferguson G, & Bense V. 2011. Uncertainty in 1D Heat-Flow Analysis to Estimate Groundwater Discharge to a Stream. *Groundwater, **49***: pp. 336-347. DOI: 10.1111/j.1745-6584.2010.00735.x.

Ferguson G, Woodbury AD, & Matile GLD. 2003. Estimating deep recharge rates beneath an interlobate moraine using temperature logs. *Groundwater, **41***: pp. 640-646.

Gonzalez-Pinzon R, Ward AS, Hatch CE, Wlostowski AN, Singha K, Gooseff MN, … & Brock JT. 2015. A field comparison of multiple techniques to quantify groundwater-surface-water interactions. *Freshwater Science, **34***: pp. 139-160. DOI: 10.1086/679738.

Gordon RP, Lautz LK, Briggs MA, & McKenzie JM. 2012. Automated calculation of vertical pore-water flux from field temperature time series using the VFLUX method and computer program. *Journal of Hydrology, **420***: pp. 142-158. DOI: 10.1016/j.jhydrol.2011.11.053.

Goto S, Yamano M, & Kinoshita M. 2005. Thermal response of sediment with vertical fluid flow to periodic temperature variation at the surface. *Journal of Geophysical Research-Solid Earth*, 110. DOI: B01106 10.1029/2004jb003419.

Hatch CE, Fisher AT, Revenaugh JS, Constantz J, & Ruehl C. 2006. Quantifying surface water-groundwater interactions using time series analysis of streambed thermal records: Method development. *Water Resources Research, **42***: pp. DOI: W10410/10.1029/2005wr004787.

Irvine DJ, Briggs MA, Lautz LK, Gordon RP, McKenzie JM, & Cartwright I. 2017a. Using Diurnal Temperature Signals to Infer Vertical Groundwater-Surface Water Exchange. *Groundwater, **55***: pp. 10-26. DOI: 10.1111/gwat.12459.

Irvine DJ, Cartwright I, Post VEA, Simmons CT, & Banks EW. 2016. Uncertainties in vertical groundwater fluxes from 1-D steady state heat transport analyses caused by heterogeneity, multidimensional flow and climate change. *Water Resources Research, **52***. DOI: 10.1002/2015WR017702.

Irvine DJ, Cranswick RH, Simmons CT, Shanafield MA, & Lautz LK. 2015b. The effect of streambed heterogeneity on groundwater-surface water exchange fluxes inferred from temperature time series. *Water Resources Research, **51***: 198-212. DOI: 10.1002/2014wr015769.

Irvine DJ, Kurylyk BL, Cartwright I, Bonham M, Post VE, Banks EW, & Simmons CT. 2017b. Groundwater flow estimation using temperature-depth profiles in a complex environment and a changing climate. *Science of The Total Environment, **574***: pp. 272-281.

Irvine DJ, Lautz LK, Briggs MA, Gordon RP, & McKenzie JM. 2015a. Experimental evaluation of the applicability of phase, amplitude, and combined methods to determine water flux and thermal diffusivity from temperature time series using VFLUX 2. *Journal of Hydrology, **531***: 728-737. DOI: 10.1016/j.jhydrol.2015.10.054.

Keery J, Binley A, Crook N, & Smith JWN. 2007. Temporal and spatial variability of groundwater-surface water fluxes: Development and application of an analytical method using temperature time series. *Journal of Hydrology,* ***336***: pp. 1-16. DOI: 10.1016/j.jhydrol.2006.12.003.

Koch FW, Voytek EB, Day-Lewis FD, Healy R, Briggs MA, Lane JW, Jr., & Werkema D. 2016. 1DTempPro V2: New Features for Inferring Groundwater/Surface-Water Exchange. *Groundwater,* ***54***: pp. 434-439.

Kurylyk BL, Irvine DJ. 2019. Heat: An Overlooked Tool in the Practicing Hydrogeologist's Toolbox. Groundwater, **57**: 517-524. DOI: 10.1111/gwat.12910.

Kurylyk BL, Irvine DJ, & Bense VF. 2019. Theory, tools, and multidisciplinary applications for tracing groundwater fluxes from temperature profiles. *Wiley Interdisciplinary Reviews-Water,* ***6***. DOI: 10.1002/wat2.1329.

Kurylyk BL, Irvine DJ, Carey SK, Briggs MA, Werkema DD, & Bonham M. 2017. Heat as a groundwater tracer in shallow and deep heterogeneous media: Analytical solution, spreadsheet tool, and field applications. *Hydrological Processes,* ***31***: pp. 2648-2661. DOI: 10.1002/hyp.11216.

Kurylyk BL, Irvine DJ, Mohammed AA, Bense VF, Briggs MA, Loder JW, & Geshelin Y. 2018. Rethinking the Use of Seabed Sediment Temperature Profiles to Trace Submarine Groundwater Flow. *Water Resources Research,* ***54***: pp. 4595-4614. DOI: 10.1029/2017wr022353.

Kurylyk BL, MacQuarrie KTB, Linnansaari T, Cunjak RA, & Curry RA. 2015. Preserving, augmenting, and creating cold-water thermal refugia in rivers: concepts derived from research on the Miramichi River, New Brunswick (Canada). *Ecohydrology,* ***8***: pp. 1095–1108. DOI: 10.1002/eco.1566.

Lautz LK. 2010. Impacts of nonideal field conditions on vertical water velocity estimates from streambed temperature time series. *Water Resources Research,* ***46***. DOI: W01509/10.1029/2009wr007917.

Lee DR. 1977. A device for measuring seepage flux in lakes and estuaries. *Limnology Oceanography,* ***22*****: pp.** 140-147. DOI: 10.4319/lo.1977.22.1.0140.

Luce CH, Tonina D, Applebee R, & DeWeese T. 2017. Was That Assumption Necessary? Reconsidering Boundary Conditions for Analytical Solutions to Estimate Streambed Fluxes. *Water Resources Research,* ***53***: pp. 9771-9790. DOI: 10.1002/2017WR020618.

Luce CH, Tonina D, Gariglio F, & Applebee R. 2013. Solutions for the diurnally forced advection-diffusion equation to estimate bulk fluid velocity and diffusivity in streambeds from temperature time series. *Water Resources Research,* ***49***: pp. 488-506. DOI: 10.1029/2012wr012380.

McCallum AM, Andersen MS, Rau GC, & Acworth RI. 2012. A 1-D analytical method for estimating surface water-groundwater interactions and effective thermal diffusivity using temperature time series. *Water Resources Research, **48***. DOI: W11532 10.1029/2012wr012007.

McCobb TD, Briggs MA, LeBlanc DR, Day-Lewis FD, & Johnson CD. 2018. Evaluating long-term patterns of decreasing groundwater discharge through a lake-bottom permeable reactive barrier. *Journal of Environmental Management*, **220**: pp. 233-245. DOI: 10.1016/j.jenvman.2018.02.083.

Modica, E. 1999. Source and age of ground-water seepage to streams. U.S. Geological Survey Fact Sheet, 063-99.

Munz M, & Schmidt C. 2017. Estimation of vertical water fluxes from temperature time series by the inverse numerical computer program FLUX-BOT. *Hydrological Processes, **31***: pp. 2713-2724. DOI: 10.1002/hyp.11198.

Murdoch LC, & Kelly SE. 2003. Factors affecting the performance of conventional seepage meters. *Water Resources Research, **39***. DOI: 10.1029/2002wr001347.

Nelder JA, & Mead R. 1965. A simplex-method for function minimization. *The Computer Journal, 7*: pp. 308-313.

Rau GC, Andersen MS, McCallum AM, Roshan H, & Acworth RI. 2014. Heat as a tracer to quantify water flow in near-surface sediments. *Earth-Science Reviews, **129***: pp. 40-58. DOI: 10.1016/j.earscirev.2013.10.015.

Rau GC, Cuthbert MO, McCallum AM, Halloran LJS, & Andersen MS. 2015. Assessing the accuracy of 1-D analytical heat tracing for estimating near-surface sediment thermal diffusivity and water flux under transient conditions. *Journal of Geophysical Research (Earth Surface)*. DOI: doi: 10.1002/2015JF003466.

Reeves J, & Hatch CE. 2016. Impacts of three-dimensional nonuniform flow on quantification of groundwater-surface water interactions using heat as a tracer. *Water Resources Research, **52***: pp. 6851-6866. DOI: 10.1002/2016WR018841.

Rosenberry DO. 2008. A seepage meter designed for use in flowing water. *Journal of Hydrology, **359***: pp. 118-130. DOI: 10.1016/j.jhydrol.2008.06.029.

Schmidt C, Conant B, Jr., Bayer-Raich M, & Schirmer M. 2007. Evaluation and field-scale application of an analytical method to quantify groundwater discharge using mapped streambed temperatures. *Journal of Hydrology, **347***: pp. 292-307. DOI: 10.1016/j.jhydrol.2007.08.022.

Schornberg C, Schmidt C, Kalbus E, & Fleckenstein JH. 2010. Simulating the effects of geologic heterogeneity and transient boundary conditions on streambed temperatures - Implications for temperature-based water flux calculations. *Advances in Water Resources, **33***: pp. 1309-1319. DOI: 10.1016/j.advwatres.2010.04.007.

Shan C, & Bodvarsson G. 2004. An analytical solution for estimating percolation rate by fitting temperature profiles in the vadose zone. *Journal of Contaminant Hydrology, **68***: pp. 83-95. DOI: 10.1016/s0169-7722(03)00126-8.

Shanafield M, Hatch C, & Pohll G. 2011. Uncertainty in thermal time series analysis estimates of streambed water flux. *Water Resources Research, **47***. DOI: W03504/10.1029/2010wr009574.

Stonestrom DA, & Blasch KW. 2003. Determining temperature and thermal properties for heat-based studies of surface-water ground-water interactions In: Heat as a Tool for Studying the Movement of Ground Water Near Streams, Stonestrom DA, & Constantz J (Eds.) USGS, pp: 73-80.

Sulis M, Meyerhoff SB, Paniconi C, Maxwell RM, Putti M, & Kollet SJ. 2010. A comparison of two physics-based numerical models for simulating surface water-groundwater interactions. *Advances in Water Resources, **33***: pp. 456-467. DOI: 10.1016/j.advwatres.2010.01.010.

Tirado-Conde J, Engesgaard P, Karan S, Muller S, & Duque C. 2019. Evaluation of Temperature Profiling and Seepage Meter Methods for Quantifying Submarine Groundwater Discharge to Coastal Lagoons: Impacts of Saltwater Intrusion and the Associated Thermal Regime. *Water*, 11(8). DOI https://doi.org/10.3390/w11081648.

Turcotte DL, & Schubert G. 2014. Geodynamics: Applications of Continuum Physics to Geological Problems. John Wiley and Sons.

Wondzell SM. 2011. The role of the hyporheic zone across stream networks. *Hydrological Processes, **25***: pp. 3525-3532. DOI: 10.1002/hyp.8119.

Zimmer MA, & Lautz LK. 2014. Temporal and spatial response of hyporheic zone geochemistry to a storm event. *Hydrological Processes, **28***: pp. 2324-2337. DOI: 10.1002/hyp.9778.